View Article Online
View Journal

Green Chemistry

Cutting-edge research for a greener sustainable future

Accepted Manuscript

This article can be cited before page numbers have been issued, to do this please use: H. A. Smith, J. Zhou and H. L. Buckley, *Green Chem.*, 2026, DOI: 10.1039/D5GC05514H.

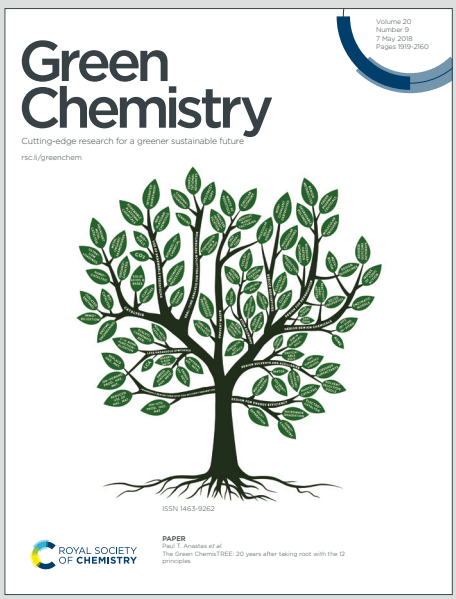

ROYAL SOCIETY OF CHEMISTRY

rsc.li/greenchem

View Article Online
DOI: 10.1039/D5GC05514H

Green Foundation

1. This work advances green chemistry by developing a safer, scalable alginate extraction process for bio-based plastics manufacturing, reducing reliance on hazardous reagents and resource-intensive processes and fossil-based polymers.
2. We demonstrate a low hazard sodium-citrate chelation method optimized through design of experiments, producing high molecular weight alginate (up to 560 kDa) with enhanced film flexibility and reductions in energy use and carbon footprint.
3. Future research will focus on closing the citrate loop through reagent recovery, trailing the established model to optimize operating conditions to produce molecular weight within the commercial range (~250 kDa) to balance yield, performance and processibility, and integrating tailored plasticizers or biopolymer blends to improve processability for high Mw applications. Model validation across varying product applications property requirement will strengthen industrial relevance.

View Article Online
DOI: 10.1039/D5GC05514H

Greener citrate-assisted extraction of sodium alginate: Process optimization and mechanical performance of alginate-based films

Hayley A. Smith[a,d], Julie Zhou[b], Heather L. Buckley[a,c,d]

[a] *Department of Civil Engineering, University of Victoria, Victoria, BC, Canada, V8P 5C2*

[b] *Department of Mathematics and Statistics, University of Victoria, Victoria, BC, Canada, V8W 2Y2*

[c] *Department of Chemistry, University of Victoria, Victoria, BC, Canada, V8W 2Y2*

[d] *Center for Advanced Materials and Related Technologies (CAMTEC), and Institute for Integrated Energy System (IESVic), University of Victoria, Victoria, BC, Canada, V8P 5C2*

(E-mail: *hayleysmith@uvic.ca*)

*corresponding author: hbuckley@uvic.ca (H.L.B.); Tel.: +1-250-472-5879

KEYWORDS

- Sodium alginate
- *Macrocystis pyrifera*
- Chelation extraction
- Sodium citrate
- Bio-based plastics
- High molecular weight
- Response surface methodology

View Article Online
DOI: 10.1039/D5GC05514H

Abstract

Alginate, a biopolymer sourced from brown seaweed, is of growing interest for bio-based materials, highlighting the need for sustainable extraction methods tailored to deliver physicochemical properties suitable for material fabrication. This work investigates a low-hazard sodium citrate chelation process that replaces multi-step extraction with a single mild-pH operation for cation removal and alginate isolation. The effects of temperature, time, and citrate concentration on yield and physicochemical properties were evaluated using Response Surface Methodology. Optimum conditions (49.5°C, 1 h, 0.125 M citrate) achieved a 21.0 ± 0.6% yield and high molecular weight (508 ± 18 kDa), a ninefold increase compared to non-optimized extraction. The method was reproducible at 20-fold scale and verified by Fourier-transform infrared spectroscopy analysis. Films derived from the optimized alginate exhibited enhanced flexibility (tensile strain = 11 ± 2%) and lower stiffness (Young's modulus = 2091 ± 236 MPa) relative to those from lower molecular weight commercial alginate. Fourier-transform infrared spectroscopy, differential scanning calorimetry, and scanning electron microscopy showed that the optimized films maintained comparable microstructural density and glass transition temperature to commercial films, with subtle differences in ionic coordination and thermal stability. In terms of environmental assessment, the optimized extraction reduced total energy use by 62% and global warming potential by 17%, compared to non-optimized. This work advances a scalable, lower impact process consistent with green chemistry principles for producing alginate suitable for bio-based plastics.

1. Introduction

Growing concerns over the environmental impacts of petroleum-based plastics, coupled with growing attention to food safety and public health, have intensified the demand for sustainable and biodegradable packaging solutions(1,2). Alginate-based materials are increasingly recognized as promising alternatives

View Article Online
DOI: 10.1039/D5GC05514H

due to their biodegradability, renewability, and compatibility with other biopolymers(3–5). Derived brown macroalgae, alginate is comprised of β-D-mannuronic acid (M) and α-L-guluronic acid (G) units arranged in block or alternating sequences(6,7). When combined with divalent cations such as calcium, alginate forms crosslinked networks, primarily through G-G blocks, forming films well-suited for a range of packaging and coating applications(8–10). Alginate functionality depends on its molecular weight and mannuronic/guluronic acid (M/G) ratio, which governs viscosity, crosslinking, and mechanical performance(11–15). These molecular properties are strongly influenced by extraction parameters, including reagent type and concentration, temperature, and reaction time, which affect depolymerization and epimerization, thereby modifying alginate structure(16).

Conventional sodium alginate extraction involves a series of processes including formaldehyde pre-treatment, acid treatment, alkali extraction, bleaching, precipitation, and drying(17). Alkaline extraction is a critical step, as it significantly affects the alginate yield, Mw, and M/G ratio(16). Sodium carbonate or sodium hydroxide is typically used to maintain pH ~11, promoting solubilization of alginate after prior acid treatment disrupts cation crosslinks in the cell wall(16). However, such strongly alkaline conditions promote β-elimination reactions that cleave glycosidic bonds, with degradation rates increasing notably above pH 10, leading to a substantial reduction in alginate molecular weight(18–20). Conventional processes also rely on hazardous reagents and high energy and water inputs, raising safety and environmental concerns(21,22). Although innovative techniques such as enzyme- and microwave-assisted extraction have emerged, their high cost and limited scalability constrain industrial near-term adoption(21). Consequently, there remains a critical need for low hazard, resource efficient extraction methods compatible with existing processing infrastructure.

Sodium citrate has emerged as a promising chelating agent for alginate extraction, enabling efficient solubilization of alginate from kelp cell walls under moderately alkaline conditions without requiring acid pre-treatment(22–24). Sodium citrate facilitates multidentate complexation with divalent cations and is a low hazard, regenerable chelating agent(22,25). Hazard assessments indicate that sodium citrate exhibits only low to moderate concerns across human and environmental endpoints(22), and is listed on the U.S.

View Article Online
DOI: 10.1039/D5GC05514H

EPA Safer Chemical Ingredients List(26). This contrasts with chemicals used in conventional acid-alkali extraction, including sodium hydroxide, sodium carbonate, and formaldehyde(22), the latter of which is regulated internationally due to its classification as a known human carcinogen and reproductive toxicity(27–29). Citrate-based extraction has also been shown to produce higher yields, improved purity, and reduced co-extraction of non-alginate components(22,24). Building on this work, recent results showed that citrate extraction can substantially reduce greenhouse gas emissions and water consumption compared to alkaline methods while maintaining high yields(22). However, the resulting alginate exhibited low molecular weights(22), despite being recovered under near-neutral pH conditions that theoretically minimize β-elimination(18,19). The reduced molecular weight compromises mechanical performance in applications such as biodegradable films(30,31).

To address these gaps, this study investigates how citrate extraction parameters govern alginate structure and performance, linking process optimization with material functionality in bio-based plastics. Response Surface Methodology (RSM) was employed to model and optimize citrate extraction from *Macrocystis pyrifera* by evaluating sodium citrate concentration, temperature, and extraction time. This design of experiments (DoE) approach reduces resource demand compared to one-factor-at-a-time trials, while capturing both individual and interactive effects of process variables(32,33). This approach has proven effective in modeling and optimizing both acid and alkaline extraction steps, enhancing the functionality of alginates for diverse applications including bio-inks, emulsifiers, and antioxidant agents(34–38), as well as other biomass valorization and modelling and optimization of greener processes(39–41). A Box-Behnken design (BBD) was employed to enhance predictive reliability by avoiding extreme conditions and ensuring robust quadratic modeling(41,42).

This work aims to maximize yield and molecular weight, validate optimal conditions experimentally, assess scalability, and evaluate environmental impact relative to non-optimized processes. Films fabricated from optimized extracts were tested for tensile properties, allowing direct benchmarking against commercial alginates and demonstrating potential for biodegradable packaging.

2. Methods and materials

View Article Online
DOI: 10.1039/D5GC05514H

2.1. Materials and reagents

Macrocystis pyrifera samples were purchased from Canadian Kelp Resources, harvested in Bamfield, British Columbia, Canada in 2023, received rinsed and dry via an air circulating oven, and used immediately after purchase. Calcium chloride 96% (anhydrous) from Acros Organics. Sodium carbonate (anhydrous) from Bio Basic Canada. Hydrochloric acid (36.5-38.0%, ACS grade), sodium citrate dihydrate >99.0%, sodium hydroxide >97.0% (ACS grade), ethanol (spectrophotometric grade; 95%), calcium carbonate >99.0% (ACS grade), calcium chloride >99.0% (ACS grade) from Fisher Chemical. Glucono-δ-lactone (food grade) from Elo's Premium. Commercial sodium alginate from KIMICA Corporation I-2 (Tokyo, Japan) (Mw = 248 kDa, M/G = 1.01). Milli-Q water was used throughout this study.

2.2. Alginate extraction

The dry kelp samples were manually broken into pieces and ground into particles of 200-600 nm using a laboratory blender. Subsequently, 1.2 g of powdered kelp was mixed with 36 g of sodium citrate solution at varying concentrations (0.1, 0.16, and 0.5 M), with each solution adjusted to pH 9.3 ± 0.1 with 1M NaOH (SevenCompact pH meter S220). The solution was mixed in an incubator shaker (New Brunswick I26 Incubator Shaker) at 150 RPM under different reaction times (1.0, 2.5, and 4.0 h) and temperatures (21.0, 35.5, and 50.0°C). Next, the mixture was centrifuged (Sorvall LYNX 4000 Superspeed Centrifuge) at 15,000 × g for 35 min at 21°C to separate the supernatant containing sodium alginate, from the solid kelp residue. The supernatant was acidified to pH 1.2 ± 0.1 with 6 M hydrochloric acid to precipitate alginic acid. The solution was vortexed for 30 s and centrifuged at 15,000 × g for 10 min at 21°C to collect the alginic acid pellet, discarding the supernatant to eliminate salts (Na^+, Mg^+), polyphenols, laminarins, and fucoidan.

The pellet was washed twice with 5 mL of 0.1 M hydrochloric acid, vortexed for 30 sec, and centrifuged at 15,000 × g for 5 min after each wash. The pellet was then resuspended in 5 mL of deionized water, neutralized to pH 7.5 with 1 M sodium carbonate, and vortexed for 3 min. Sodium alginate was

View Article Online
DOI: 10.1039/D5GC05514H

precipitated by adding anhydrous ethanol (1:1, v/v), followed by centrifugation at 15,000 × g for 10 min at 21°C. The pellet was washed with 5 mL of 70% ethanol (1:1, v/v) and centrifuged for 5 min. The final sodium alginate extract was oven-dried at 40°C until a constant weight was achieved. The dried extract was milled using a Retsch Laboratory Mixer Mill MM 400 equipped with a 25 mL steel ball canister at 30 Hz for 30 s. Milled samples were refrigerated in vials for future use. The yield of sodium alginate was calculated using Equation (1).

$$Yield\ (\%) = \frac{Dry\ wt.\ of\ extract\ (g)}{Dry\ wt.\ of\ algal\ biomass\ (g)} \times 100 \quad (1)$$

2.3. NMR spectroscopy analysis

The uronic acid composition of sodium alginate was determined using variable temperature Nuclear Magnetic Resonance Spectroscopy (^{1}H NMR) on a Bruker DMX-500 MHz instrument at 85°C. A 2% solution of sodium alginate was prepared in deuterium oxide (D_2O) and analyzed in 5 mm NMR tubes (43). The spectra were processed using MestReNova software (Mnova), focusing on the relative integrations of three resonance peaks, which correspond to distinct chemical environments. These integrations were used to calculate the fractions of guluronic acid (G-blocks) and mannuronic acid (M-blocks), M/G ratio, based on established equations (44,45).

2.4. Molecular weight determination

The molecular weight distribution of sodium alginate samples was characterized using Gel Permeation Chromatography (GPC). The analysis employed a Waters 2695 separation module coupled with a DAWN HELEOS-II multiangle laser light scattering (MALLS) detector and an Optilab T-rEX refractive index detector. Separation was achieved using Waters Ultrahydrogel HPLC columns, including a guard, linear, and 120 columns. The mobile phase consisted of 10 mM phosphate-buffered 0.1 M $NaNO_3$ at pH 7. Key parameters such as molecular weight distribution, weight-average molecular weight (Mw), number-average molecular weight (Mn) and polydispersity index (Mw/Mn) were determined to comprehensively characterize the alginate samples.

View Article Online
DOI: 10.1039/D5GC05514H

2.5. Modeling and optimization using RSM

This study employed a Box-Behnken design within the response surface methodology (RSM) framework to evaluate and optimize the effects of extraction time (X_1), temperature (X_2), and sodium citrate concentration (X_3) on alginate yield, M/G ratio, and molecular weight. The design was generated using State-Ease 360 software (Version 2023, State-Ease Inc., USA) and included 12 factorial and 5 center points, totaling 17 experimental runs. Sodium citrate concentration was modeled on a logarithmic scale to account for nonlinear behavior across a wide range, emphasizing lower levels commonly reported in literature(22,24,46,47). The corresponding sodium citrate concentrations were 0.05 M (low, $10^{-1.3}$), 0.16 M (center, $10^{-0.8}$), and 0.50 M (high, $10^{-0.3}$). Table 1 summarizes the experimental ranges and coded levels for each variable (factor).

Table 1. Independent factors and coded levels used in the BBD.

Factor Label	Factor	Range of Factors		
		Low-level (-1)	Center-level (0)	High-level (+1)
X_1	Time (h)	1.0	2.5	4.0
X_2	Temperature (°C)	21.0	35.5	50.0
X_3	Log [Sodium Citrate (M)]	-1.30 (0.05 M)	-0.80 (0.16M)	-0.30 (0.50 M)

The design assessed various combinations of the factors, and a quadratic polynomial model in Equation (2) was used to describe the response functions (Y) in relation to the process factors (48).

$$Y = \beta_o + \sum \beta_i X_i + \sum \beta_{ii} X_i^2 + \sum \beta_{ij} X_i X_j + \varepsilon, \quad (2)$$

where, β_0 is the regression intercept, and β_i, β_{ii}, and β_i□ are unknown coefficients for the linear (X_i), quadratic (X_i^2), and interaction (X_iX_j) effects, and ε represents the experimental error. The significance of each term in the regression equation was assessed.

2.6. Up-scaled sodium alginate extraction

The upscaled extraction was performed at a 20-fold increase relative to the laboratory-scale procedure (Section 2.2), using the optimized conditions identified in Section 3.4. Ground kelp (24 g) was mixed

View Article Online
DOI: 10.1039/D5GC05514H

with 720 g of 0.125 M sodium citrate (pH 9.3 ± 0.1) and agitated at 150 rpm for 1 h at 49.5°C. After extraction, solids were removed by centrifugation (15,000 × g, 30 min, 21°C), and the supernatant was acidified to pH 1.2 ± 0.2 with 6 M HCl to precipitate alginic acid. The precipitate was collected by centrifugation (15,000 × g, 10 min) and washed twice with 0.1 M HCl (100 mL per wash).

The washed alginic acid was redissolved by dispersing in Milli-Q water and neutralizing to pH 7.5 ± 0.2 with Na_2CO_3 under stirring (350 rpm, 20 min). Sodium alginate was then precipitated with anhydrous ethanol (1:1 v/v; ~100 mL), isolated by centrifugation (15,000 × g, 10 min), and washed twice with 70% ethanol (100 mL per wash). Drying, milling, and storage were conducted as described in Section 2.2.

2.7. FTIR spectroscopy analysis

Fourier Transform Infrared Spectroscopy (FTIR) was used to (i) confirm the characteristic chemical structure of sodium alginate extracted via the optimized upscaled process and compare it to commercial sodium alginate, and (ii) evaluate Ca^{2+} carboxylate coordination in crosslinked alginate films as a spectroscopic indicator of relative ionic crosslink density.

Spectra were collected using a Cary 630 FTIR spectrometer (Agilent Technologies) over the 4000-450 cm^{-1} wavenumber range, with 64 scans at a spectral resolution of 4 cm^{-1}. Commercial sodium alginate was analyzed as a reference material to verify characteristic alginate absorption bands. FTIR measurements were performed in triplicate for extracted alginate samples and for each film formulation.

2.8. Preparation of alginate films

Plasticized films were fabricated from two sodium alginate sources: (i) material obtained via the up-scaled optimized extraction developed in this study and (ii) commercial alginate (KIMICA, Tokyo, Japan). A 2% (w/v) sodium alginate suspension was prepared by dissolving 5.0 g of sodium alginate in 250 mL Milli-Q water. The solution was homogenized with a lab blender, and the suspension was left overnight to allow entrained air to dissipate from the solution. Next, 140 g of the alginate suspension was mixed with 0.8% (w/v) mannitol, which served as a plasticizer, and 0.82 g glucono-δ-lactone. Separately, 0.23

View Article Online
DOI: 10.1039/D5GC05514H

g $CaCO_3$ was dispersed in 5 mL water and combined with the alginate solution under stirring for 20 minutes to ensure homogenous dispersion. The resulting uniform suspension was portioned into 35 g aliquots and cast into 150 x 15 mm Petri dishes. The Petri dished were covered and allowed to internally gel for 24 h at 21°C. Crosslinking was achieved by adding 70 mL of 66.67 mM $CaCl_2$ containing 0.8% (w/v) mannitol. After 30 min in the crosslinking solution, the films were rinsed three times with Milli-Q water. To minimize edge curling during drying, films were pinned along their perimeters onto plastic wrapped boards and air dried at 21°C for 3 days. Dried films were laser-cut into 7 x 1 cm rectangular tensile samples, prepared according to ASTM D882 standards for tensile properties of plastic films (49).

2.9. Film Characterization

2.9.1 Mechanical analysis and measurement of film thickness

Prior to testing, all rectangular samples were conditioned at 23°C and 50% relative humidity for 24 h. Tensile properties were evaluated using a universal testing machine (INSTRON 5565, Norwood, MA, USA), equipped with pneumatic grips and operated at 1 mm/min.

Film thickness was measured at three random points per film, using a digital micrometer caliper (General Ultra-Tech, NY). For each film type, six replicates were tested. Bluehill 3 software (Instron) was used to calculate tensile strength, elongation at break, and Young's modulus from the load-extension data. The mean values were reported for each film type.

2.9.2. Film moisture content

Film moisture content (M_c, %) was determined gravimetrically. Samples were conditioned at 23°C and 50% humidity for 24 hours, then dried at 105°C until a constant weight was achieved. The average moisture content from three replicates was calculated using Equation (3):

$$M_c\,(\%) = \frac{(W_0 - W_d)}{W_0} * 100 \qquad (3)$$

Where, W_0 represents the conditioned weight, and W_d is the dry weight.

View Article Online
DOI: 10.1039/D5GC05514H

2.9.3. Film cross-section microstructure

The microstructure of film cross-sections using scanning electron microscopy (Hitachi S-4800). Dried film samples were lyophilized for 22 h to remove residual moisture, then fractured with forceps to obtain clean cross-sectional breaks. Fractured segments (approximately 5×3 mm) were stored in a desiccator prior to analysis. For imaging, samples were mounted on 90° aluminum specimen stubs and sputter-coated with a 10-20 nm layer of gold. Cross-sectional images were observed using an accelerating voltage of 1 kV. Three replicates were completed at magnification of 10x and 100x.

2.9.4. Film thermal properties

Differential scanning calorimetry (DSC) was performed using a TA Instruments DSC 25 (TA Instruments, New Castle, DE, USA) under a nitrogen purge. Film samples (4-6 mg) were sealed in hermetic aluminum pans, with an empty hermetic pan used as the reference. To remove residual moisture that may obscure the glass transition, samples were first lyophilized. They were then subjected to a preheating cycle from 20 to 60°C at 10°C min^{-1}, followed by cooling to 10°C. The second heating cycle, used for analysis, was conducted from 10 to 300°C at 10°C min^{-1}. At least three measurements were performed for each film type to ensure reproducibility. The glass transition temperature (T_g), onset degradation temperature, and primary exothermic peak temperatures were calculated from the second heating cycle using TRIOS software (TA Instruments, New Castle, DE, USA).

2.10. Statistical analysis

Statistical analysis results, including p-values, F-values, lack-of-fit tests, R^2, adjusted R^2, and diagnostic plots, were assessed to determine the most suitable model for modelling the experimental data. RSM modeling and statistical analysis were performed using Design-Expert v22 software (Stat-Ease 360). A one-way ANOVA was conducted to compare the yield, M/G ratio, and molecular weight of extracted alginate among the model predictions, validation experiment, and upscaled extraction. Tukey's post hoc test was performed in OriginPro 2023 to identify pairwise differences among the RSM-predicted optimized, validated optimized, and upscaled optimized conditions.

View Article Online
DOI: 10.1039/D5GC05514H

2.11. Environmental impact assessment

This assessment quantified the chemical, energy, and water demands of alginate extraction to evaluate environmental trade-offs between non-optimized and optimized citrate extraction processes. The analysis focused on chemical, energy, and water consumption, as well as global warming potential (GWP), using a functional unit of 1 kg sodium alginate. Gate-to-gate boundaries included all extraction steps, with yield standardized across methods. Process data were derived from experimental conditions in this study and from Smith et al. (2024) for the non-optimized process, with aligned precipitation and purification steps. Energy requirements for heating, mixing, and solid-liquid separation was estimated through an upscaling scenario using literature-based industrial data, following the same scope and assumptions as Smith et al. (2024). Drying, milling, equipment manufacture, and transport were excluded for consistency with prior assessment. Global warming potential was determined using the ReCiPe Midpoint (H) 2016 method in openLCA(50) with Ecoinvent v3.5 inventory data(51). The datasets, assumptions and calculations are detailed in the Supplementary Information.

3. Results and discussion

In this study, sodium citrate-assisted extraction of alginate from *Macrocystis pyrifera* was investigated using RSM. A BBD was applied to model and optimize the effects of extraction time, temperature, and sodium citrate concentration on extraction efficiency and key alginate properties. In the sections that follow, the model is validated and analyzed to assess the influence of process conditions on response variables. Additional experiments were performed at predicted optimal conditions to verify model accuracy. Finally, the optimized process was scaled up and alginate films were developed to investigate mechanical properties.

3.1. Modelling and statistical analysis of data using response surface methodology

The performance and validity of the fitted response surface models were evaluated through diagnostic analyses of experimental data for alginate yield and physicochemical properties. Experimental values for

View Article Online
DOI: 10.1039/D5GC05514H

alginate recovery, M/G ratio, and molecular weight under the BBD are presented in Table 2. Detailed uronic acid composition is provided in the Supplementary information (Table S1).

Table 2. Box–Behnken experimental design showing treatment conditions and corresponding observed responses for sodium alginate extraction.

Std. Order	Factors			Responses						
	X_1: Time (h)	X_2: Temp. (°C)	X_3: Sodium Citrate (M)	Yield (% DW)	M/G ratio	Fraction of GG blocks, F_{GG}	Fraction of MM blocks, F_{MM}	Weight avg. Mw, Mw (kDa)	Number avg. Mw, Mn (kDa)	Polydispersity Index, PDI (M_n/M_w)
1	1	21	0.16	17.67	1.11	0.21	0.27	327	214	1.53
2	4	21	0.16	17.01	1.02	0.23	0.24	246	164	1.50
3	1	50	0.16	19.32	1.15	0.25	0.32	403	366	1.10
4	4	50	0.16	18.36	0.84	0.25	0.16	343	208	1.65
5	1	35.5	0.05	15.68	1.19	0.19	0.28	287	197	1.46
6	4	35.5	0.05	18.35	0.82	0.28	0.18	168	115	1.46
7	1	35.5	0.5	9.82	1.41	0.17	0.34	210	129	1.62
8	4	35.5	0.5	12.61	1.11	0.23	0.28	120	77	1.56
9	2.5	21	0.05	14.40	1.44	0.17	0.35	223	145	1.54
10	2.5	50	0.05	16.59	1.17	0.22	0.30	274	202	1.36
11	2.5	21	0.5	4.68	1.49	0.16	0.36	174	99	1.75
12	2.5	50	0.5	10.75	1.52	0.16	0.37	232	154	1.51
13	2.5	35.5	0.16	17.57	0.89	0.23	0.17	255	151	1.68
14	2.5	35.5	0.16	20.58	0.94	0.26	0.23	258	212	1.22
15	2.5	35.5	0.16	19.84	1.02	0.26	0.27	219	141	1.55
16	2.5	35.5	0.16	18.32	1.00	0.22	0.22	327	208	1.58
17	2.5	35.5	0.16	19.05	0.96	0.24	0.22	280	166	1.68

Sodium citrate concentration is presented in logarithmic form; see Table 1 for details. DW, denotes dry weight.

Using the data presented in Table 2, a quadratic model (Equation 2) was fitted for the three response variables (yield, MW, M/G ratio). The three independent variables (X_1, X_2, and X_3) were coded at levels of −1, 0, and 1. Residual analysis was subsequently conducted to evaluate the adequacy of each model. Diagnostic plots were used to evaluate the effectiveness of the regression model. Fig. 1a shows the normal probability plot of externally studentized residuals for yield and M/G ratio, which closely follows a linear trend, confirming the assumption of normality (i.e., that residuals are normally distributed). However, the normal probability plot for molecular weight displayed noticeable deviations from linearity (Supplementary Information, Fig. S1.), suggesting a non-normal distribution. A natural logarithmic

View Article Online
DOI: 10.1039/D5GC05514H

transformation was applied to the molecular weight data, which resulted in a close-to-linear trend, thereby justifying the necessity of data transformation to satisfy normality assumptions.

The relationship between the predicted response values and externally studentized residuals is displayed in Fig. 1b. The random distribution of residuals across the predicted values supports the assumption of homoscedasticity, indicating that the residual variance is constant across the range of model predictions. No significant outliers were identified, as observed in the diagnostic plots. Furthermore, the parity plot (Fig. 1c) comparing predicted versus experimental response values demonstrates that data points align closely with the 45-degree reference line, indicating strong agreement between the model and experimental observations.

View Article Online
DOI: 10.1039/D5GC05514H

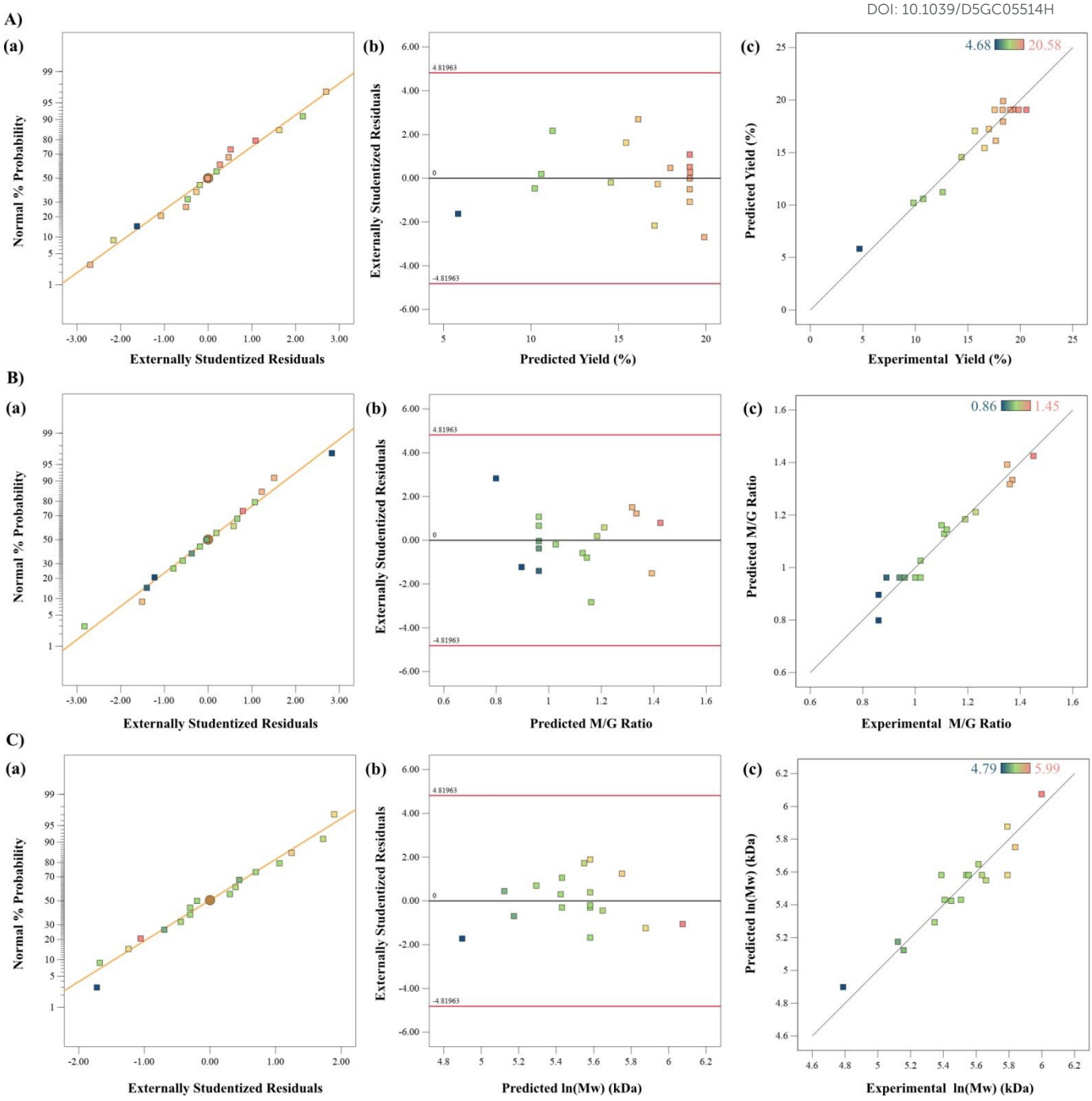

Fig. 1. Diagnostic plots of A) alginate yield, B) M/G ratio and C) molecular weight; a) normal plot of externally studentized residuals, b) relationship between the predicted response variables and externally studentized residuals, c) comparison of the predicted and experimental values of response variables.

The experimental relationship between independent factors and response variables, estimated from the data obtained using Box-Behnken design, are represented by quadratic polynomial equations below:

$$\text{Yield (\%)} = 19.07 + 0.48X_1 + 1.41X_2 - 3.40X_3 + 0.76{X_1}^2 - 1.75{X_2}^2 - 5.72{X_3}^2 - 0.08X_1X_2 + 0.03X_2X_3 + 0.97X_1X_3 \quad (4)$$

View Article Online
DOI: 10.1039/D5GC05514H

$$\text{M/G ratio} = 0.96 - 0.13X_1 - 0.05X_2 + 0.09X_3 - 0.05X_1^2 + 0.13X_2^2 + 0.23X_3^2 - 0.06X_1X_2 + 0.04X_2X_3 + 0.03X_1X_3 \quad (5)$$

$$\ln(\text{Mw}) = 5.58 - 0.19X_1 + 0.13X_2 - 0.13X_3 + 0.01X_1^2 + 0.19X_2^2 - 0.37X_3^2 + 0.03X_1X_2 + 0.02X_2X_3 - 0.01X_1X_3 \quad (6)$$

where, X_1, X_2 and X_3 represents the coded factors for extraction time, temperature, and sodium citrate concentration, respectively. The interpretation and analysis of these equations are given below.

Table 3. Analysis of variance (ANOVA) for the models in Equations (4), (5) and (6) of alginate yield, M/G ratio and molecular weight.

Source	DF	Yield				M/G ratio				ln(Mw)			
		Sum of squares	Mean square	F-value	p-value	Sum of squares	Mean square	F-value	p-value	Sum of squares	Mean square	F-value	p-value
Model	9	269.71	29.97	12.08	0.0017	0.55	0.06	16.32	0.0007	1.26	0.14	6.69	0.0101
X_1 – Time	1	1.84	1.84	0.74	0.4173*	0.14	0.14	36.05	0.0001	0.2962	0.2962	14.16	0.007
X_2 – Temp.	1	15.85	15.85	6.39	0.0394	0.02	0.02	5.60	0.0498	0.1342	0.1342	6.42	0.0391
X_3 – Conc.	1	92.21	92.21	37.16	0.0005	0.06	0.06	16.80	0.0046	0.1411	0.1411	6.75	0.0356
X_1X_2	1	0.02	0.02	0.01	0.9268*	0.02	0.02	4.17	0.081*	0.0038	0.0038	0.1801	0.684*
X_1X_3	1	0.00	0.00	0.00	0.9707*	0.00	0.00	0.81	0.399*	0.0001	0.0001	0.0052	0.9445*
X_2X_3	1	3.76	3.76	1.52	0.2579*	0.00	0.00	1.31	0.291*	0.0018	0.0018	0.0842	0.7801*
X_1^2	1	2.46	2.46	0.99	0.3528*	0.01	0.01	2.64	0.148*	0.0006	0.0006	0.0304	0.8566*
X_2^2	1	12.84	12.84	5.17	0.0571*	0.07	0.07	18.68	0.0035	0.1516	0.1516	7.25	0.031
X_3^2	1	137.81	137.81	55.54	0.0001	0.22	0.22	58.87	0.0001	0.5598	0.5598	26.76	0.0013
Residual	7	17.37	2.48			0.03	0.00			0.1464	0.0209		
Lack of Fit	3	11.68	3.89	2.74	0.1774*	0.02	0.01	2.01	0.255*	0.0597	0.0199	0.9187	0.508*
Pure Error	4	5.69	1.42			0.01	0.00			0.0867	0.0217		
Model statistics													
R^2		0.94				0.96				0.90			
Adj. R^2		0.86				0.90				0.76			
Adeq. Precision		11.65				13.33				10.60			
C.V%		9.90				5.53				2.63			

X_1, X_2, and X_3 denote coded factors for time, temperature, and sodium citrate concentration, respectively; R^2 is the coefficient of determination, and C.V. % is the percentage coefficient of variation.
* Not significant (p-value > 0.05).

Analysis of variance (ANOVA) was performed to evaluate the statistical significance and accuracy of the estimated model and the individual terms, as shown in Table 3. The model exhibited high F-values, which leads to small p-values (< 0.05), for alginate yield (12.08), M/G ratio (16.32), and molecular weight (7.38) indicating that the variation in the response can be explained by the regression model. The lack-of-fit test assessed whether the model accurately represents the relationship between response and predicted values. A p-value > 0.05 indicates no significant lack-of-fit, supporting a good model fit.

Model accuracy was assessed using the coefficient of determination (R^2), where values approaching 1.0 indicate a strong model fit. The R^2 values were 0.94 for yield, 0.96 for the M/G ratio, and 0.90 for

View Article Online
DOI: 10.1039/D5GC05514H

molecular weight, suggesting a strong correlation between the model and experimental data. The models explained 93.95%, 95.45%, and 89.59% of the variations in yield, M/G ratio, and molecular weight, respectively, under the given extraction conditions, with only small variations (6.05%, 4.55%, and 10.41%) attributed to random or unexplained experimental errors.

Adequate precision, which quantifies the signal-to-noise ratio, exceeded the minimum threshold of 4 for all models, confirming sufficient discrimination between signal and background noise. Furthermore, the coefficient of variation (C.V.), used to assess model reproducibility, was determined to be 9.90% for yield, 5.53% for the M/G ratio, and 2.15% for molecular weight, indicating high precision and reliability in the regression model predictions.

To investigate refinement of the model, an iterative backward elimination approach was applied, where model terms with p-values exceeding 0.100 were considered statistically insignificant. The analysis showed that removing these terms had negligible impact on the model's predictive capability, as the optimization conditions and predicted results remained unchanged. Consequently, all model terms were retained in the regression analysis. Overall, the statistical evaluations confirmed good regression model fit and suitability for modeling and optimization.

3.2. Influence of process conditions on alginate yield and its physicochemical properties

Response surface plots (Fig. 2) were used to analyze interaction effects between independent variables on yield, M/G ratio, and molecular weight. These plots were generated from the fitted model equations, with other variables held at their central values (BBD center level 0 in Table 1) to visualize the interaction between each pair. For instance, by maintaining the extraction time at 2.5 h (Fig. 2Ac) the interaction between chelate concentration, temperature and the resultant yield can be visualized across their studied ranges.

View Article Online
DOI: 10.1039/D5GC05514H

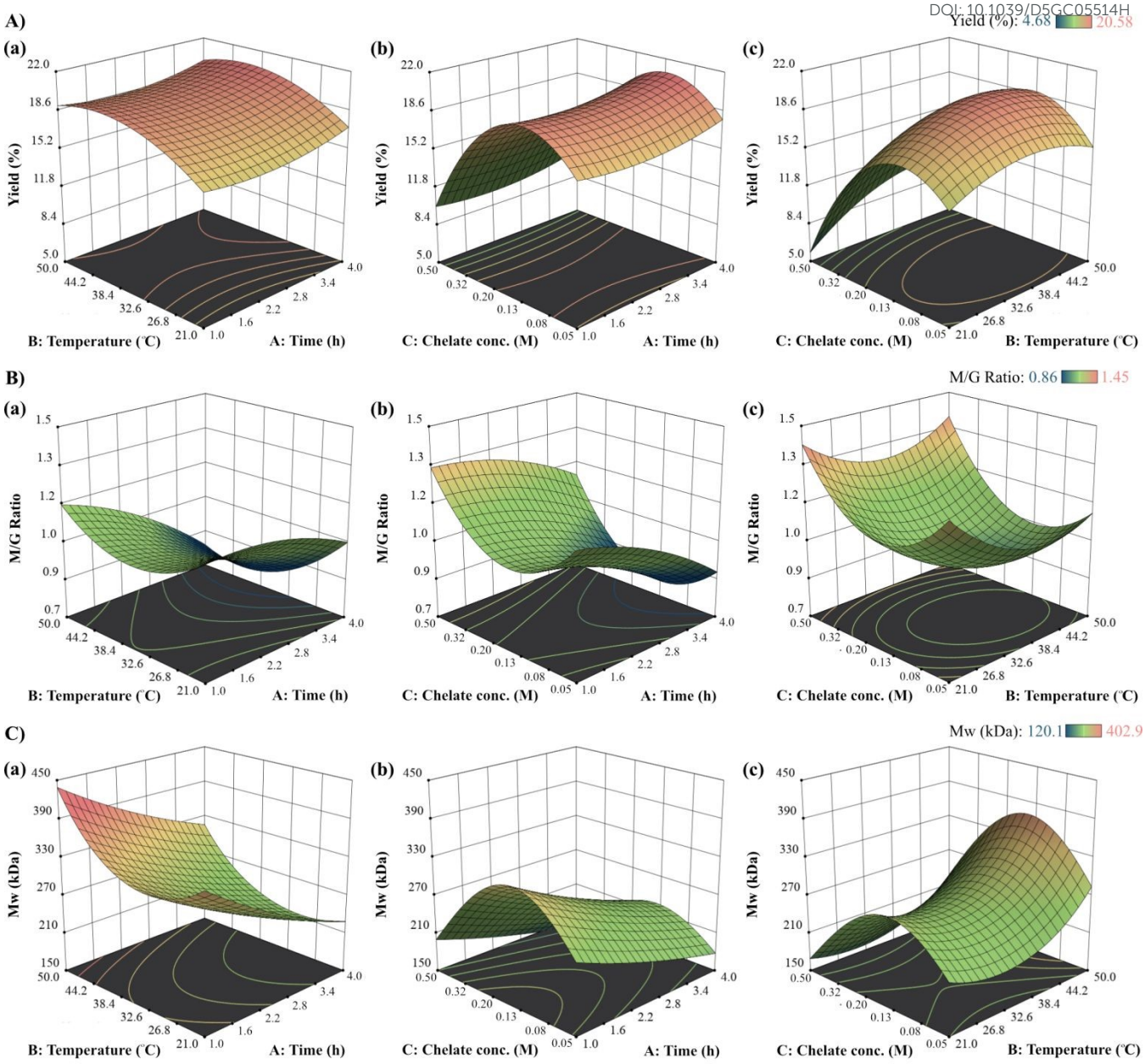

Fig. 2. Response surface plots showing the effects of extraction time, temperature, and sodium citrate concentration (chelate conc.) on A) alginate yield, B) M/G ratio, and C) molecular weight of sodium alginate extracted from *Macrocystis pyrifera*.

3.2.1. Effect of operation parameters on alginate yield

Sodium alginate yield ranged from 4.68% to 20.53% (Fig. 2A). Among the factors examined, chelate concentration had the most significant influence (p-value = 0.0005), with a significant quadratic term (p-value = 0.0001) was observed demonstrating a trend of maximal yield near the center-level concentration, then reduced as concentration approached low and high concentrations (Fig. 2A). Low concentrations likely provided insufficient chelation to disrupt divalent cation crosslinks in the algal matrix, while high concentrations may degrade alginate or promote side reactions.

View Article Online
DOI: 10.1039/D5GC05514H

Temperature also significantly influenced yield (p-value = 0.0394), with higher temperatures promoting greater recovery of alginate. These observations align closely with findings from previous studies that demonstrated improved extraction efficiency at higher temperatures, attributed primarily to reductions in viscosity and enhanced mass transfer across cell walls (6,52–54). Extraction time exhibited minimal influence on alginate yield within the experimental range tested. Supplementary Information (Fig. S2.) provides details from pre-screening experiments, indicating longer extraction time of 16 h improved the alginate recovery. No significant interaction effects were detected among variables, indicating their independent contributions to yield.

3.2.2. Effect of process conditions on uronic acid composition

The M/G ratios ranged from 0.86 to 1.46 (Fig.2B), with GG block fractions (FGG) between 0.16-0.28 and MM block fractions (FMM) between 0.16–0.37. Extraction time showed the strongest linear effect (p-value = 0.0005), where longer durations resulted in lower M/G ratios (higher G content). This likely reflects the progressive release of Ca^{2+} cross-linked G-blocks, which are more tightly bound within the cell wall matrix. As yield increased, G-block content also increased (lower M/G), as shown in Supplementary Information (Fig. S3.). Partial hydrolysis of M-blocks during extended extractions may further contribute to the shift, consistent with reports of alginate cleavage into mono- and dicarboxylic acids(55,56). Temperature and chelating agent concentration exhibited significant quadratic effects (p-value = 0.0022 and p-value = 0.0001, respectively), with lower M/G ratios observed near the midpoint of the tested ranges and higher values at both low and high extremes (Fig. 2B). This non-linear trend may reflect a balance between alginate release and degradation. No significant interaction effects were indicated between process variables.

3.2.3. Influence of process conditions on molecular weight

Sodium alginate molecular weight ranged from 174 to 403 kDa (Fig. 2C). The Mw was significantly influenced by extraction time, temperature, and citrate concentration (Fig. 2C). Extraction time exhibited

View Article Online
DOI: 10.1039/D5GC05514H

the strongest influence (p-value = 0.0071), with longer extraction times reducing Mw, particularly at elevated temperatures and 0.16 M citrate (Fig. 2C). This is consistent with depolymerization observed in pre-screening (Supplementary Information Fig. S2.) and prior studies reporting decreased viscosity and reduced molecular weight, attributed to alginate depolymerization under extended extraction (58,59). Temperature significantly influenced Mw (p-value = 0.0391), with higher temperatures resulting in increased Mw. Moreover, citrate concentration exhibited a significant quadratic effect on Mw (p-value = 0.0013), with a maximum Mw at 0.13 M (Fig. 2Cb and Fig. 2Cc). Concentrations above or below this optimum led to a sharp decrease in Mw, with values dropping to as low as 171 kDa, independent of extraction time and temperature. Excessive citrate may enhance chain degradation, whereas insufficient citrate may not remove divalent cations, hindering extraction of alginate.

3.3. Optimization of design parameters and validation of the model

Derringer's desirability function was applied to integrate multiple response variables and identify extraction conditions that simultaneously maximize alginate yield and molecular weight. This approach effectively combines model predictions to achieve optimal process settings (Table 4). In this study, maximizing yield and molecular weight was prioritized due to their strong influence on the mechanical and functional performance of alginate-based materials, while the M/G ratio was targeted near 1 to approximate the balanced composition of commercial alginate. Molecular weight, in particular, is a critical determinant of film strength, elasticity, and solubility. Prior studies have shown that alginate films with higher molecular weights (~300 kDa) exhibit enhanced mechanical strength and reduced solubility relative to lower molecular weight fractions (< 200 kDa)(30,31). Although elevated molecular weight can lead to increased viscosity and processing challenges (60), this trade-off is well recognized in polymer systems and can be mitigated through formulation modifications. The positive correlation between molecular weight and mechanical performance is well established across both natural and synthetic polymers, including cellulose derivatives and polyethylene, where chain entanglement enhances tensile strength and durability(61,62). Reports specifically examining high molecular weight alginate films,

View Article Online
DOI: 10.1039/D5GC05514H

particularly those containing plasticizers, remain limited, highlighting the need for further research into the relationship between molecular weight, and end-use functionality.

Using Derringer's desirability function analysis, the optimal conditions for maximizing alginate yield and molecular weight were determined to be an extraction time of 1 h, temperature of 49.5°C, and sodium citrate concentration of 0.125 M. Under these conditions, the model predicted a yield of 19.42%, the M/G ratio of 1.17, and a Mw of 436 kDa (Table 5). The composite desirability achieved a score of 0.963 (where 1 represents full desirability)(63).

Table 4. Objectives and parameter settings used in Derringer's desirability function analysis for multi-response optimization of alginate extraction conditions.

Conditions for Response Variable	Goal	Target	Lower Limit	Upper Limit	Importance
Yield (%)	Maximize	-	4.68	20.58	3.00
M/G Ratio	Target	1.00	0.86	1.45	1.00
Weight avg. Mw, Mw (kDa)	Maximize	-	120.10	402.90	3.00

Triplicate experiments conducted under optimized conditions validated the model's accuracy (Table 5). The experimental alginate yield ($21.03 \pm 0.60\%$) was slightly higher than the predicted value, with a relative error of 7.6%. No significant difference was observed between the predicted and experimental means, confirming the model's accuracy for yield prediction. Similarly, the molecular weight obtained experimentally was 508.07 ± 18.70 kDa, with a 14% relative error and no significant difference from the predicted value, established by Tukey's test (p-value > 0.05), further supporting the model's reliability. Notably, this optimized molecular weight obtained in this study is relatively high for *Macrocystis pyrifera*, exceeding the typical range reported in the literature, which generally spans from 94 to 297 kDa (22,64–66). The only study reporting a higher Mw (700 kDa) involved the use of hazardous chemical, formaldehyde, an known carcinogen (28,67). Furthermore, the experimental M/G ratio of 0.95 ± 0.03 exhibited a 23% relative error and a statistically significant difference from the predicted value, indicating limitations in the model's ability to predict the uronic acid composition.

View Article Online
DOI: 10.1039/D5GC05514H

Table 5. Comparison of sodium alginate extracted from *Macrocystis pyrifera* under non-optimized, predicted optimized, validated optimized, and upscaled optimized conditions. Reported values include average yield, uronic acid composition, block structure parameters, molecular weight, and polydispersity index.

	Avg. Yield (% DW)	M/G ratio	Fraction of GG blocks, F_{GG}	Fraction of MM blocks, F_{MM}	Fraction of alternating MG, GM blocks, $F_{GM,MG}$	G Block length, $\overline{N_G}$	M Block length, $\overline{N_M}$	Block distribution, η	Weight avg. Mw, Mw (kDa)	Number avg. Mw, Mn (kDa)	Polydisper Index, PI (M_n/M_w
Model Prediction	19.42 ± 1.57[a]	1.17 ± 0.06[a]	-	-	-	-	-	-	435.81 ± 63.37[a]	-	-
Validation Optimized*	21.03 ± 0.60[a]	0.95 ± 0.03[b]	0.21 ± 0.03	0.18 ± 0.02	0.30 ± 0.02	1.70 ± 0.14	1.61 ± 0.10	1.21 ± 0.09	508.07 ± 18.70[a, b]	441.87 ± 21.13	1.15 ± 0.0
Upscaled Optimized*	19.78 ± 0.44[a]	0.96 ± 0.00[b]	0.19 ± 0.02	0.17 ± 0.03	0.32 ± 0.02	1.59 ± 0.12	1.52 ± 0.12	1.29 ± 0.10	559.50 ± 26.27[b]	508.73 ± 27.05	1.10 ± 0.0
Non-optimized (22)	26.70 ± 0.58	0.63 ± 0.03	0.34 ± 0.01	0.11 ± 0.04	0.27 ± 0.03	2.27 ± 0.07	1.42 ± 0.06	1.16 ± 0.04	59.50 ± 13.30	38.5 ± 11.0	2.20 ± 1.5

Data are presented as mean ± standard deviation (n = 3). DW, denotes dry weight.
Data with different letters within a column indicate significant differences among the mean values (Tukey's test, p-value < 0.05).

4. Upscaled optimized sodium alginate extraction

To assess scalability and reproducibility, alginate extraction was conducted under upscaled conditions equivalent to 20-fold the validation scale (Section 2.6), processing 24 g of dried, ground *Macrocystis pyrifera*. The resulting alginate yield and physicochemical characteristics were compared to both validation-scale and model-predicted results (Table 5).

Under upscaled optimized conditions, the yield, M/G ratio, and molecular weight were statistically comparable to validation-scale results, confirmed by Tukey's test (p-value > 0.05). These findings indicate that the extraction process is reproducible and maintains alginate physicochemical properties at larger scales. The upscaled experimental yield closely aligned with the model prediction, while significant differences were observed between upscaled and predicted values for molecular weight and uronic acid composition. The higher than predicted molecular weight obtained during upscaling (559.5 kDa) may reflect that the optimized point lies near the boundary of the Box-Behnken design space, where extrapolation is less reliable and response curvature is more pronounced. Incorporating additional experimental points or expanding the design space would likely improve predictive accuracy.

View Article Online
DOI: 10.1039/D5GC05514H

Additionally RSM development at a scale closer to the intended production volume may reduce scale-dependent effects and further refine model predictability.

Compared to the non-optimized extraction (16 h at room temperature using 0.2 M sodium citrate), using a different *Macrocystis pyrifera* sample(22), the optimized and upscaled extractions yielded alginate with a substantially increased molecular weight (Mw from 59.50 kDa to 508.07-560.50 kDa) and a narrower molecular weight distribution (PDI = 1.10-1.15). A lower polydispersity index indicates reduced polymer chain degradation and more uniform molecular size distribution(68,69). Both the validation and upscaled optimized processes yielded lower alginate recovery, likely due to the shorter extraction time, consistent with the influence of extraction duration on yield discussed in Section 3.3.1.

4.1. FTIR spectroscopy analysis of sodium alginate

The FTIR spectrum of sodium alginate from the optimized upscaled extraction process was analyzed and compared to commercial sodium alginate (Fig. 3). The spectral analysis showed characteristic absorption bands indicative of alginate's structure. A broad band at 1600-1610 cm^{-1} corresponded to the asymmetric stretching of the carboxylate group (O-C-O)(70), while the band at 1400–1428 cm^{-1} was associated with C-OH deformation coupled with the symmetric stretching of O-C-O4(71,72). The band at 1025-1030 cm^{-1} confirmed the presence of C-O groups, and the distinctive bands in the anomeric region (950-750 cm^{-1}), characteristic of carbohydrate structures, was present(70,73). Peaks at 930-950 cm^{-1} were indicative of uronic acid presence by the C-O stretching vibration(74), whereas a peak at 883 cm^{-1} was linked to C1-H deformation in β-mannuronic acid residues. Further, peaks within the 815-833 cm^{-1} range were associated with mannuronic acid residues(55,74).

The fingerprint region of the optimized upscaled sodium alginate spectrum exhibited strong alignment with the commercial reference, with characteristic absorption bands appearing at similar positions. These findings confirm that sodium alginate is the predominant polysaccharide in the extracted product.

View Article Online
DOI: 10.1039/D5GC05514H

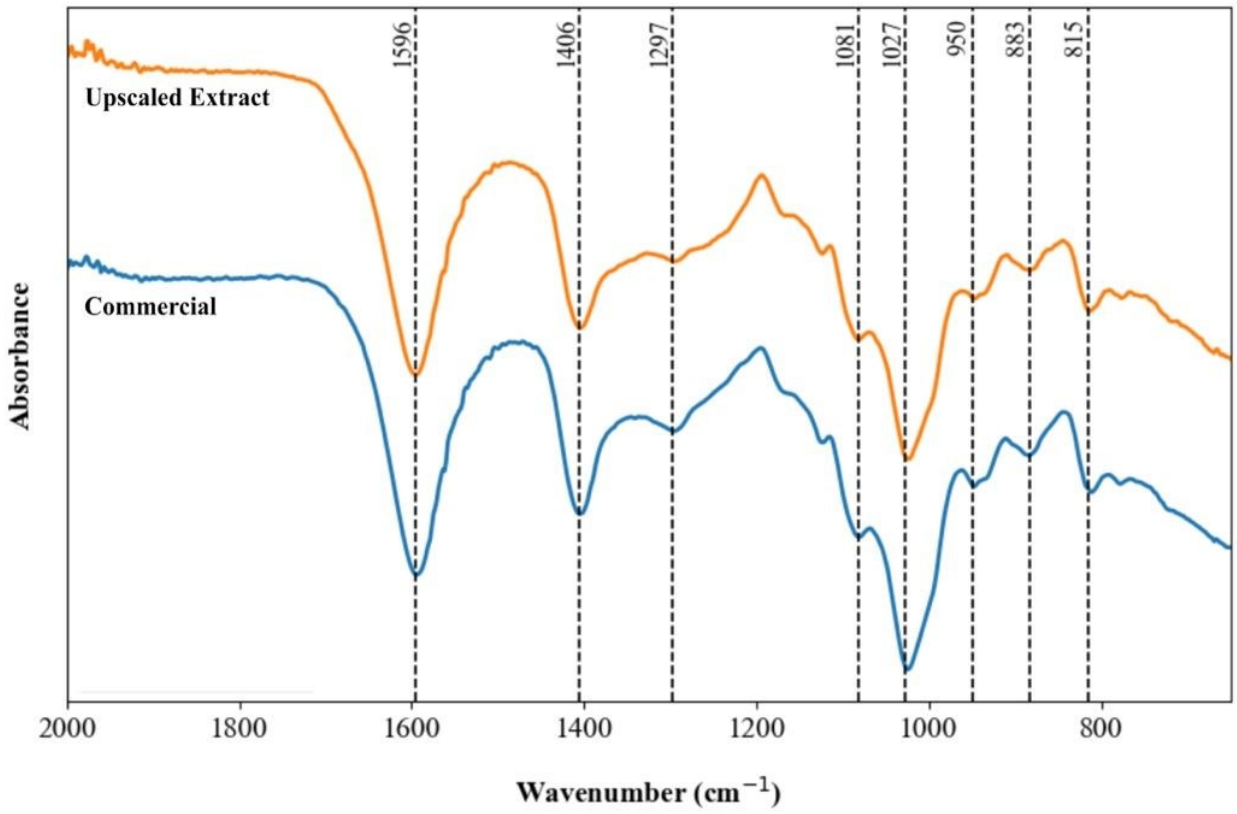

Fig. 3. FTIR spectra of sodium alginate extracted using the optimized method, compared with the commercial sodium alginate reference (KIMICA, Tokyo, Japan).

5. Film characterization

5.1. Mechanical properties

To evaluate the mechanical performance of alginate films derived from the optimized extraction (Opt-Film), tensile strength, Young's modulus, and elongation at break were measured and benchmarked against films produced from commercial sodium alginate (Com-Film; Mw = 248 kDa, M/G = 1.01, detailed commercial uronic acid block composition outlined in the Supplementary Information; Table S2). The Opt-Film had an average thickness of 80 µm compared to 60 µm for the Com-Film. Moisture contents were comparable at 11.4% and 11.6%, respectively (Table 6).

Table 6. Mechanical properties of alginate-based films prepared from upscaled optimized extract and commercial alginate (KIMICA, Tokyo, Japan).

Film Type	Thickness (µm)	Moisture (%)	Youngs Modulus (MPa)	Tensile Stress (MPa)	Tensile Strain (%)

View Article Online
DOI: 10.1039/D5GC05514H

Commercial (Com-Film)	60 ± 4	11.6 ± 1.2	3732 ± 526	104 ± 48	9.2 ± 2
Upscaled and Optimized (Opt-Film)	80 ± 6	11.4 ± 0.7	2091 ± 236	66 ± 8	11 ± 2

Values are presented as mean ± standard deviation (n = 6).

The Com-Film displayed a mean Young's modulus of 3732 MPa, tensile strength of 104 MPa, and elongation at break of 9.2%. The Opt-Film exhibited correspondingly lower modulus and strength (2091 MPa and 66 MPa), while the elongation at break was 11%. These data indicate that the Opt-Film formed a mechanically less rigid and less strong material but can sustain slightly greater deformation prior to failure.

Prior studies similarly document molecular weight dependent trends. Costa et al. (2018) reported that Ca^{2+}crosslinked films derived from higher Mw alginates displayed greater elongation at break, yet higher tensile strength and modulus relative to lower molecular weight formulations(30). Avella et al. (2007), using non-crosslinked alginate films, observed reduced stress, modulus, and strain at break in films prepared from higher Mw alginate compared to lower Mw, and noted that increasing glycerol content further decreased stiffness(75). Interpretation across studies is constrained by differences in uronic acid composition, which strongly influences network architecture. G-block-rich alginates typically form more rigid junction zones, whereas M-block rich structures yield more flexible backbones due to their glycosidic bond orientation. The present results reinforce the need for controlled, systematic evaluation of molecular weight effects, decoupled from uronic acid composition, on the mechanical and thermal performance of alginate films.

5.2. FTIR spectroscopy analysis of films

FTIR spectroscopy was used to evaluate Ca^{2+} carboxylate coordination in the films, providing a spectroscopic indicator of relative crosslink density. FTIR spectra of films showed the characteristic asymmetric (ν_{asym}) and symmetric (ν_{sym}) COO^- stretching for both film types (Table 7).

Table 7. FTIR carboxylate symmetric and asymmetric vibrational frequencies for Com-Films and Opt Films.

View Article Online
DOI: 10.1039/D5GC05514H

Film Type	ν(COO)sym	ν(COO)asym	Δν
Com-Film	1408.93 ± 2.64	1590.64 ± 1.32	181.71 ± 1.32
Opt-Film	1405.83 ± 1.08	1594.06 ± 1.8	188.23 ± 1.86

Values are mean ± standard deviation (n = 3). $\Delta\nu = (\nu_{asym} - \nu_{sym})$.

The shifts were observed in both bands, with Com-Films showing greater shifts compared to Opt-Films. The smaller band difference, Δν, has been associated with stronger coordinated Ca^{2+} carboxylate interactions and denser polymer networks(72,76–78). The Δν for Com-Films was 182 cm^{-1} and Opt-Films was 188 cm^{-1}, indicating a less densely packed ionic network and fewer or more loosely organized junction zones in Opt-Films. These results align with the mechanical results, where Com-Films displayed higher stiffness and tensile strength, while Opt-Films showed lower rigidity and slightly higher strain at break.

5.3. Differential scanning calorimetry analysis

DSC was used to determine the glass transition temperature and thermal stability of the films (Table 8), thermographs shown in Supplementary Information. Samples from both film types exhibited a glass transition of approximately 88°C, indicating similar chain mobility between Opt-Film and Com-Film. The T_g values measured here are higher than those reported for alginate films containing greater moisture or different plasticizers, consistent with literature showing that water lowers T_g by increasing chain mobility(79,80), and mannitol as a plasticizer results in a higher T_g than other plasticizers (i.e., glycerol, sorbitol, or isomalt)(81).

Table 8. Differential Scanning Calorimetry parameters for Com-Film and Opt-Film.

Film Type	Tg (°C)	Thermal Onset Degradation (°C)	Primary Exothermic Peak (°C)
Com-Film	88.43 ± 0.54	219.35 ± 2.61	239.08 ± 3.91
Opt-Film	88.49 ± 0.42	217.77 ± 0.74	259.26 ± 2.82

Reported values are mean ± standard deviation (n = 3).

A broad endothermic event centered near 140°C was observed for both film types and corresponds to water evaporation(79). A distinct endothermic peak at 218-219°C appeared in all thermograms, likely associated with cleavage of calcium-carboxyl crosslinks(79,82,83). At higher temperatures, an

View Article Online
DOI: 10.1039/D5GC05514H

exothermic peak associated with alginate thermal oxidation was detected in both films(84). The Com-Film showed an average exothermic peak at 239°C, whereas the Opt-Film showed greater thermal stability, exhibiting a higher temperature peak at 259°C. The higher temperature exotherm is consistent with the elevated molecular weight of the extracted alginate, which can delay thermal breakdown through increased chain entanglement(85). The onset thermal degradation and exothermal peak align within similar ranges with prior reports for calcium-alginate films(75,79), with the Opt-Film showing greater exothermic peak temperatures. Coupled DSC and thermogravimetric analysis (TGA) is recommended to confirm mass loss events associated with each thermal transition.

5.4. Scanning electron microscopy

SEM cross-sectional images (Fig. 4) showed that both films formed compact and homogeneous structures with only minor defects. Slightly more porous edge regions were observed for the Com-Film, while the Opt-Film maintained more uniform density across the cross-section. These dense and homogeneous features are consistent with reports of alginate films prepared under low-moisture conditions and with limited plasticizer content(75,86–89).

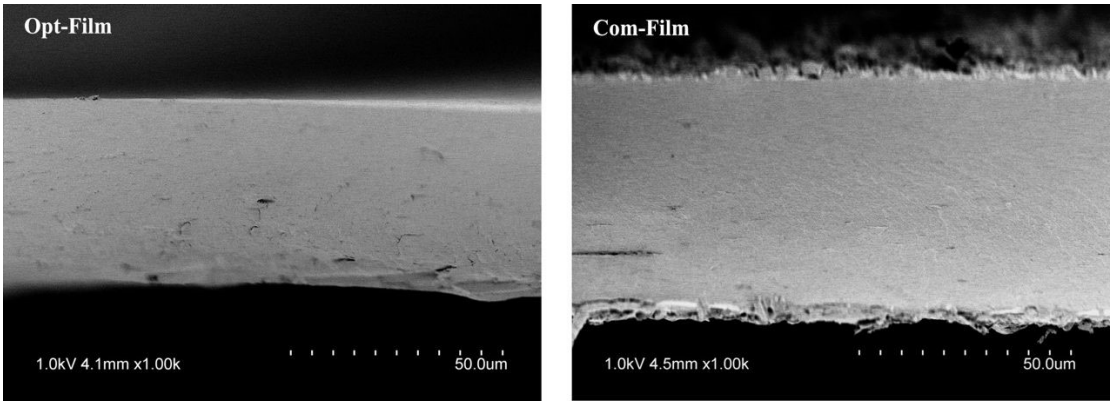

Figure 4. Cross-sectional SEM images of Opt-Film and Com-Film at 1000× magnification, showing dense structures with minor defects. The Opt-Film exhibits more uniform density compared to the slightly more porous edge region of the Com-Film.

5.5. Effect of molecular weight on film properties

The two films displayed similar uronic acid compositions, so the observed differences in mechanical response, COO^- band separation, and thermal behavior likely are from the higher molecular weight of the optimized extract (559.5 kDa, nearly two-fold of commercial alginate). Higher molecular weight alginates

View Article Online
DOI: 10.1039/D5GC05514H

increase solution viscosity, enhance intermolecular entanglement, and strengthen chain-chain interactions, contributing to cohesive films even when ionic crosslink density is lower. Higher molecular weight alginates exhibit reduced gelling rates due to slower chain diffusion during gelation(90).

As expected for high molecular weight alginate solutions, the Opt-Film formulation exhibited greater viscosity during film casting, which can constrain processability(60). The use of tailored plasticizers (e.g., glycerol, sorbitol, essential oils) or blending with compatible biopolymers may mitigate these limitations(75,81,91,92). Nevertheless, high molecular weight alginate may be advantageous in alternative applications, such as alginate-based fibre production(93–95), surface coatings, and composite films(66,96). Future work should further investigate sodium alginate extraction optimizing alginate molecular weight within the commercial range (~250 kDa), using a desirability function approach to balance yield and performance. This would enable direct comparison of the extracted alginate to commercial standards and facilitate tuning of mechanical properties for specific applications.

6. Environmental assessment

A comparative environmental analysis was performed to assess energy, material, and emissions impacts of the optimized upscaled versus non-optimized sodium citrate extractions. The assessment revealed notable improvements in all three categories for the optimized process (Table 9). Full data inventory, calculations, sources, assumptions are provided in the Supplementary Information.

Table 9. Resource consumption (chemical and energy) and global warming contributions for optimized and non-optimized citrate-based alginate extractions, normalized to 1 kg of sodium alginate product at equivalent yield.

Parameters and Impacts		Optimized (This study) (kg CO_2-eq)	Non-optimized (adapted from Smith et al., 2024) (kg CO_2-eq)
Inputs	Energy (MJ)		
	Heating (MJ) (natural gas)	17.10	-
	Electricity (MJ)	40.06	149.71
	Freshwater (L)	196.98	196.98
	Ethanol (96%) (L)	51.78	51.78
	Hydrochloric acid (30% soln) (L)	10.71	10.71
	Sodium carbonate (kg)	1.12	1.12
	Sodium citrate (kg)	4.89	7.83
	Sodium hydroxide (kg)	0.06	0.06
	Energy (total)	3.76	4.13

View Article Online
DOI: 10.1039/D5GC05514H

Impact on Climate Change (kg CO_2-eq)	Heating (natural gas)	2.66	-
	Electricity	1.10	4.13
	Freshwater	0.30	0.30
	Ethanol	54.96	54.96
	Hydrochloric acid	1.23	1.23
	Sodium carbonate	0.51	0.51
	Sodium citrate	29.43	47.08
	Sodium hydroxide	0.08	0.08
	Total	90.26	108.28

Reducing the mixing duration from 16 h to 1 h decreased electricity consumption from 149.7 MJ to 40.1 MJ, representing the main driver of improved total energy efficiency. Although the optimized method introduced mild heating at 49.5°C (17.1 MJ from natural gas), this addition was negligible compared with the energy savings from reduced mixing. The optimized process also required less sodium citrate (0.125 M vs 0.2 M), further decreasing chemical demand. Sodium citrate remained the dominant contributor to chemical-related impacts, yet showed the largest change, decreasing from 47.1 kg CO_2-eq in the non-optimized to 29.4 kg CO_2-eq in the optimized process, a 38% reduction. Still, the sodium citrate impact on climate change underscores the need to enable circular use. Sodium citrate regeneration and reuse present a promising approach to reduce resource demand and global-warming potential, as shown by Sterner and Edlund(25). Overall, total GWP decreased from 108.3 kg CO_2-eq to 90.3 kg CO_2-eq, a 20% decrease, reflecting reduced electricity and sodium citrate consumption. The optimized extraction achieved lower total energy consumption, reduced chemical input, and decreased emissions despite the additional heating requirement.

Compared with conventional multi-step alginate extractions reported in prior studies, the optimized citrate process exhibits markedly lower energy intensity and carbon footprint. Conventional protocols typically involve sequential pre-treatment, acid-mediated cation removal, and multi-stage alkaline extraction, leading to energy demands exceeding 140 MJ kg^{-1} of product and elevated freshwater use due to repeated washing and processing steps(22). The citrate-based approach consolidates these steps into a single mild-pH operation, eliminating corrosive reagents and reducing water inputs. Furthermore, assessments of alkaline extractions without formaldehyde pre-treatment reported GWP values of 987.23 kg CO_2-eq and

View Article Online
DOI: 10.1039/D5GC05514H

389.81 kg CO_2-eq per kg of sodium alginate(22), considerably higher than the values calculated here. Although formaldehyde is commonly used in alginate pre-treatment(21), its environmental impacts have received limited life cycle evaluation. Mohammed et al. (2023) quantified chemical contributions for alginate extraction involving formaldehyde and reported substantial environmental impacts associated with Na_2CO_3, methanol, NaOCl, H_2SO_4, and formaldehyde used in pre-treatment, and noted that wastewater streams contain elevated sulfate concentrations from acid and bleaching steps(97). Their study did not account for end-of-life treatment of formaldehyde containing waste; which under U.S. EPA's Resource Conservation and Recovery Act and Clean Water Act regulations, these wastes must be managed as hazardous, which can add additional processing and disposal requirements(29). These contextual differences highlight the comparatively lower material and energy intensity of the citrate-based extraction evaluated in this work.

Furthermore, citrate-based alginate extraction can be implemented using standard industrial equipment, lowering capital investment requirements and adoption barriers. Emerging green technologies, such as microwave- or ultrasound-assisted extraction rely on high cost systems, with concern of commercial-scale feasibility(21). The practical scalability positions the optimized citrate-based extraction process as a more feasible pathway toward lower impact, industrial alginate production.

7. Conclusion

Chelate-assisted extraction of sodium alginate from *Macrocystis pyrifera* was successfully modelled and optimized using a Box–Behnken design, identifying temperature, extraction time, and sodium citrate concentration as key variables affecting yield, M/G ratio, and Mw. Citrate concentration was the most influential factor, with both insufficient and excessive concentrations reducing yield and producing low Mw alginate. Extended extraction time increased G-block content but reduced Mw. Optimal conditions (49.5°C, 1 h, 0.125 M citrate) produced alginate with high yield (21.0%) and a Mw of 508 kDa, among the highest reported for *Macrocystis pyrifera*, and were reproducible at 20-fold scale-up. In terms of environmental performance, the optimized citrate extraction reduced total energy consumption by 62% and global warming potential by 17% relative to the non-optimized process. These improvements were

View Article Online
DOI: 10.1039/D5GC05514H

driven by shorter mixing time and lower reagent concentration, with minimal trade-offs observed aside from increase in heating energy.

Films fabricated from the optimized alginate exhibited improved flexibility compared to commercial reference. FTIR indicated reduced Ca^{2+} crosslink density, and DSC showed similar T_g but higher thermal stability for the Opt-films, observations that correspond with the measured mechanical differences. SEM demonstrated comparable cross-sectional density. Together, this research provides valuable insight into greener citrate-assisted extraction and demonstrates how RSM can be used to tailor alginate yield and physicochemical properties. By controlling these structural parameters, material properties can be tuned to enable application specific alginate procedures for use in packaging, food, biomaterials, and advanced functional products.

Corresponding author

Heather L. Buckley – Department of Civil Engineering, Centre for Advanced Materials and Related Technologies (CAMTEC) and Institute for Integrated Energy System (IESVic), University of Victoria, Victoria, BC, Canada, V8P 5C2

E-mail: hbuckley@uvic.ca

https://orcid.org/0000-0001-7147-0980

Present addresses

Hayley A. Smith - Department of Civil Engineering, Centre for Advanced Materials and Related Technologies (CAMTEC) and Institute for Integrated Energy System (IESVic), University of Victoria, Victoria, BC, Canada, V8P 5C2 https://orcid.org/0000-0001-6385-8037

Julie Zhou - Department of Mathematics and Statistics, University of Victoria, Victoria, BC, Canada, V8W 2Y2. E-mail: jzhou@uvic.ca

Author contributions

View Article Online
DOI: 10.1039/D5GC05514H

Hayley A. Smith, Conceptualization, Data curation, Methodology, Formal analysis, Investigation, Software, Writing - Original draft. **Julie Zhou,** Validation, Writing - Review & Editing, **Heather L. Buckley,** Supervision, Funding acquisition, Writing - Review & Editing.

Funding sources

This project was funded by Mitacs Accelerate, Bioform Technologies, NSERC Discovery, Canadian Foundation for Innovation JELF, BCKDF.

Conflicts of interest

The authors declare no competing financial interest.

Data availability

The authors confirm that the data supporting the findings of this study are available within the article and its Supplementary Information (SI), which includes additional figures (normality assessment, preliminary extraction trials, and M/G-yield correlation), and environmental assessment data, sources, assumptions and calculations for optimized and non-optimized citrate extractions.

Acknowledgment

We acknowledge and respect the Lək^{w}əŋən (Songhees and X^{w}sepsəm/Esquimalt) Peoples on whose territory the university stands, and the Lək^{w}əŋən and W̱SÁNEĆ Peoples whose historical relationships with the land continue to this day. We gratefully acknowledge the collaboration with Bioform Technologies, and extend special thanks to Dr. Jordan MacKenzie and Dr. Zhaoyang Yuan for their mentorship. We thank Nathan Leonard for his assistance in developing the film fabrication method. We also appreciate the support of CAMTEC, and Dr. Chris Barr, all of whom have played important roles in advancing this research.

Appendix A. Supplementary data

Supplementary material

References

View Article Online
DOI: 10.1039/D5GC05514H

1. Petkoska AT, Daniloski D, D'Cunha NM, Naumovski N, Broach AT. Edible packaging: Sustainable solutions and novel trends in food packaging. Food Res Int. 2021;140:109981.

2. Rosenboom JG, Langer R, Traverso G. Bioplastics for a circular economy. Nat Rev Mater. 2022 Feb 1;7(2):117–37.

3. Rai P, Mehrotra S, Priya S, Gnansounou E, Sharma SK. Recent advances in the sustainable design and applications of biodegradable polymers. Bioresour Technol. 2021;325:124739.

4. Vijayalakshmi K, Latha S, Rose MH, Sudha P. Industrial applications of alginate. In: Industrial applications of marine biopolymers. CRC press; 2017. p. 545–75.

5. Zhang C, Show PL, Ho SH. Progress and perspective on algal plastics – A critical review. Bioresour Technol. 2019 Oct;289:121700.

6. Torres MR, Sousa AP, Silva Filho EA, Melo DF, Feitosa JP, de Paula RC, et al. Extraction and physicochemical characterization of Sargassum vulgare alginate from Brazil. Carbohydr Res. 2007;342(14):2067–74.

7. Lee KY, Mooney DJ. Alginate: properties and biomedical applications. Prog Polym Sci. 2012;37(1):106–26.

8. Cazón P, Velazquez G, Ramírez JA, Vázquez M. Polysaccharide-based films and coatings for food packaging: A review. Food Hydrocoll. 2017 July;68:136–48.

9. Li H, Wang Z, Zhu F, Li G. Alginate-based active and intelligent packaging: Preparation, properties, and applications. Int J Biol Macromol. 2024 Nov 1;279:135441.

10. Tammina SK, Priyadarshi R, Khan A, Manzoor A, Rahman RSHA, Banat F. Recent developments in alginate-based nanocomposite coatings and films for biodegradable food packaging applications. Int J Biol Macromol. 2025 Mar 1;295:139480.

11. Ching SH, Bansal N, Bhandari B. Alginate gel particles–A review of production techniques and physical properties. Crit Rev Food Sci Nutr. 2017 Apr 13;57(6):1133–52.

12. Draget KI, Skjåk-Bræk G, Smidsrød O. Alginate based new materials. Int J Biol Macromol. 1997;21(1–2):47–55.

13. Zhao X, Li B, Xue C, Sun L. Effect of molecular weight on the antioxidant property of low molecular weight alginate from Laminaria japonica. J Appl Phycol. 2012;24:295–300.

14. Szekalska M, Puciłowska A, Szymańska E, Ciosek P, Winnicka K. Alginate: current use and future perspectives in pharmaceutical and biomedical applications. Int J Polym Sci. 2016;2016(1):7697031.

15. Li JW, Dong S, Song J, Li CB, Chen XL, Xie BB, et al. Purification and characterization of a bifunctional alginate lyase from Pseudoalteromonas sp. SM0524. Mar Drugs. 2011;9(1):109–23.

16. Bojorges H, López-Rubio A, Martínez-Abad A, Fabra MJ. Overview of alginate extraction processes: Impact on alginate molecular structure and techno-functional properties. Trends Food Sci Technol. 2023 Oct 1;140:104142.

17. McHugh DJ. A guide to the seaweed industry. 2003;

View Article Online
DOI: 10.1039/D5GC05514H

18. Donati I, Paoletti S. Material properties of alginates. Alginates Biol Appl. 2009;1–53.

19. Haug A, Smidsrod O, Larsen B. Degradation of alginates at different pH values. Acta Chem Scand. 1963;17(5):1466.

20. Haug A. Composition and properties of alginates. Compos Prop Alginates. 1964;

21. Saji S, Hebden A, Goswami P, Du C. A brief review on the development of alginate extraction process and its sustainability. Sustainability. 2022;14(9):5181.

22. Smith HA, Cabling LPB, Leonard NA, Dubrawski KL, Buckley HL. Green Alginate Extraction from Macrocystis pyrifera for Bioplastic Applications: Physicochemical, Environmental Impact, and Chemical Hazard Analyses. ACS Sustain Resour Manag. 2024;

23. Rahelivao MP, Andriamanantoanina H, Heyraud A, Rinaudo M. Structure and properties of three alginates from Madagascar seacoast algae. Food Hydrocoll. 2013;32(1):143–6.

24. Sterner M, Edlund U. Multicomponent fractionation of Saccharina latissima brown algae using chelating salt solutions. J Appl Phycol. 2016 Aug;28(4):2561–74.

25. Sterner M, Ribeiro MS, Gröndahl F, Edlund U. Cyclic fractionation process for Saccharina latissima using aqueous chelator and ion exchange resin. J Appl Phycol. 2017 Dec;29(6):3175–89.

26. US EPA O. Safer Chemical Ingredients List [Internet]. 2013 [cited 2025 Dec 11]. Available from: https://www.epa.gov/saferchoice/safer-ingredients

27. Registration Dossier - ECHA [Internet]. [cited 2025 Dec 11]. Available from: https://echa.europa.eu/registration-dossier/-/registered-dossier/15858/7/1

28. Pharos P. Pharos. [cited 2025 June 16]. Formaldehyde (CASRN 50-00-0) — chemical profile. Available from: https://pharos.habitablefuture.org/chemicals/2008361

29. US EPA O. Laws and Regulations Concerning Formaldehyde [Internet]. 2013 [cited 2025 Dec 10]. Available from: https://www.epa.gov/formaldehyde/laws-and-regulations-concerning-formaldehyde

30. Costa MJ, Marques AM, Pastrana LM, Teixeira JA, Sillankorva SM, Cerqueira MA. Physicochemical properties of alginate-based films: Effect of ionic crosslinking and mannuronic and guluronic acid ratio. Food Hydrocoll. 2018 Aug;81:442–8.

31. Liling G, Di Z, Jiachao X, Xin G, Xiaoting F, Qing Z. Effects of ionic crosslinking on physical and mechanical properties of alginate mulching films. Carbohydr Polym. 2016 Jan 20;136:259–65.

32. Box GE, Wilson KB. On the experimental attainment of optimum conditions. In: Breakthroughs in statistics: methodology and distribution. Springer; 1992. p. 270–310.

33. Witek-Krowiak A, Chojnacka K, Podstawczyk D, Dawiec A, Bubała K. Application of response surface methodology and artificial neural network methods in modelling and optimization of biosorption process. Spec Issue Biosorption. 2014 May 1;160:150–60.

34. Fawzy MA, Gomaa M, Hifney AF, Abdel-Gawad KM. Optimization of alginate alkaline extraction technology from Sargassum latifolium and its potential antioxidant and emulsifying properties. Carbohydr Polym. 2017 Feb;157:1903–12.

View Article Online
DOI: 10.1039/D5GC05514H

35. Fawzy MA, Gomaa M. Optimization of citric acid treatment for the sequential extraction of fucoidan and alginate from Sargassum latifolium and their potential antioxidant and Fe (III) chelation properties. J Appl Phycol. 2021;33(4):2523–35.

36. Lorbeer AJ, Lahnstein J, Bulone V, Nguyen T, Zhang W. Multiple-response optimization of the acidic treatment of the brown alga Ecklonia radiata for the sequential extraction of fucoidan and alginate. Bioresour Technol. 2015;197:302–9.

37. Mohammed A, Rivers A, Stuckey DC, Ward K. Alginate extraction from Sargassum seaweed in the Caribbean region: Optimization using response surface methodology. Carbohydr Polym. 2020;245:116419.

38. Yamashita C, Moraes ICF, Ferreira AG, Branco CCZ, Branco IG. Multi-response optimization of alginate bleaching technology extracted from brown seaweeds by an eco-friendly agent. Carbohydr Polym. 2021;251:116992.

39. Glasson CRK, Donnet L, Angell A, Vucko MJ, Lorbeer AJ, Vamvounis G, et al. Multiple response optimisation of the aqueous extraction of high quality ulvan from Ulva ohnoi. Bioresour Technol Rep. 2019 Sept 1;7:100262.

40. Hu D, Xu R, Jin Y, Sun S, Ye J, Wu J, et al. Green and sustainable extraction of phycocyanin from Spirulina platensis by temperature-sensitive polymer-based aqueous two-phase system and mechanism study. Bioresour Technol. 2024 Sept 1;407:131142.

41. Mishra A, Sawood GM, Gautam SB, Trivedi RK. Optimization of process inputs for the synthesis of waste rice bran oil isolated Pseudomonas aeruginosa MTCC 424 biosurfactant using response surface methodology for oil recovery applications. Bioresour Technol Rep. 2021 June 1;14:100653.

42. Myers RH, Montgomery DC, Anderson-Cook CM. Response surface methodology: process and product optimization using designed experiments. John Wiley & Sons; 2016.

43. Sellimi S. Structural, physicochemical and antioxidant properties of sodium alginate isolated from a Tunisian brown seaweed. Int J Biol Macromol. 2015;10.

44. Grasdalen H. High-field, 1H-n.m.r. spectroscopy of alginate: sequential structure and linkage conformations. Carbohydr Res. 1983 July;118:255–60.

45. Grasdalen H, Larsen B, Smidsrød O. A p.m.r. study of the composition and sequence of uronate residues in alginates. Carbohydr Res. 1979 Jan 1;68(1):23–31.

46. Albers E, Malmhäll-Bah E, Olsson J, Sterner M, Mayers JJ, Nylund GM, et al. Influence of preservation methods on biochemical composition and downstream processing of cultivated Saccharina latissima biomass. Algal Res. 2021 May;55:102261.

47. Sterner M, Edlund U. High-Performance Filaments from Fractionated Alginate by Polyvalent Cross-Linking: A Theoretical and Practical Approach. Biomacromolecules. 2018 Aug 13;19(8):3311–30.

48. Bezerra MA, Santelli RE, Oliveira EP, Villar LS, Escaleira LA. Response surface methodology (RSM) as a tool for optimization in analytical chemistry. Talanta. 2008;76(5):965–77.

49. ASTM D. Standard test method for tensile properties of thin plastic sheeting. Annu Book ASTM Stand. 2018;8:182–90.

View Article Online
DOI: 10.1039/D5GC05514H

50. Ciroth A. ICT for environment in life cycle applications openLCA—A new open source software for life cycle assessment. Int J Life Cycle Assess. 2007;12:209–10.

51. Wernet G, Bauer C, Steubing B, Reinhard J, Moreno-Ruiz E, Weidema B. The ecoinvent database version 3 (part I): overview and methodology. Int J Life Cycle Assess. 2016;21:1218–30.

52. Hifney AF, Fawzy MA, Abdel-Gawad KM, Gomaa M. Industrial optimization of fucoidan extraction from Sargassum sp. and its potential antioxidant and emulsifying activities. Food Hydrocoll. 2016;54:77–88.

53. Xia Y, Kuang H, Yang B, Wang Q, Liang J, Sun Y, et al. Optimum extraction of acidic polysaccharides from the stems of Ephedra sinica Stapf by Box–Behnken statistical design and its anti-complement activity. Carbohydr Polym. 2011;84(1):282–91.

54. Mohammed A, Bissoon R, Bajnath E, Mohammed K, Lee T, Bissram M, et al. Multistage extraction and purification of waste Sargassum natans to produce sodium alginate: An optimization approach. Carbohydr Polym. 2018;198:109–18.

55. Chandía NP, Matsuhiro B, Mejías E, Moenne A. Alginic acids in Lessonia vadosa: partial hydrolysis and elicitor properties of the polymannuronic acid fraction. J Appl Phycol. 2004;16(2):127–33.

56. Aida TM, Kumagai Y, Smith RL. Mechanism of selective hydrolysis of alginates under hydrothermal conditions. J Bioresour Bioprod. 2022 Aug 1;7(3):173–9.

57. Vauchel P, Kaas R, Arhaliass A, Baron R, Legrand J. A new process for extracting alginates from Laminaria digitata: reactive extrusion. Food Bioprocess Technol. 2008;1:297–300.

58. Truus K, Vaher M, Taure I. Algal biomass from Fucus vesiculosus (Phaeophyta): investigation of the mineral and alginate components. Proc Est Acad Sci Chem. 2001;50(2):95–103.

59. Vauchel P, Arhaliass A, Legrand J, Kaas R, Baron R. DECREASE IN DYNAMIC VISCOSITY AND AVERAGE MOLECULAR WEIGHT OF ALGINATE FROM LAMINARIA DIGITATA DURING ALKALINE EXTRACTION 1. J Phycol. 2008;44(2):515–7.

60. LeRoux MA, Guilak F, Setton LA. Compressive and shear properties of alginate gel: effects of sodium ions and alginate concentration. J Biomed Mater Res Off J Soc Biomater Jpn Soc Biomater Aust Soc Biomater Korean Soc Biomater. 1999;47(1):46–53.

61. Aswathy S, NarendraKumar U, Manjubala I. The influence of molecular weight of cellulose on the properties of carboxylic acid crosslinked cellulose hydrogels for biomedical and environmental applications. Int J Biol Macromol. 2023;239:124282.

62. Rahman MS, Hasan MS, Nitai AS, Nam S, Karmakar AK, Ahsan MS, et al. Recent developments of carboxymethyl cellulose. Polymers. 2021;13(8):1345.

63. Derringer G, Suich R. Simultaneous optimization of several response variables. J Qual Technol. 1980;12(4):214–9.

64. Gomez CG, Pérez Lambrecht MV, Lozano JE, Rinaudo M, Villar MA. Influence of the extraction–purification conditions on final properties of alginates obtained from brown algae (Macrocystis pyrifera). Int J Biol Macromol. 2009 May;44(4):365–71.

View Article Online
DOI: 10.1039/D5GC05514H

65. Peteiro C. Alginate Production from Marine Macroalgae, with Emphasis on Kelp Farming. In: Rehm BHA, Moradali MF, editors. Alginates and Their Biomedical Applications [Internet]. Singapore: Springer; 2018 [cited 2023 Aug 3]. p. 27–66. (Springer Series in Biomaterials Science and Engineering). Available from: https://doi.org/10.1007/978-981-10-6910-9_2

66. Hurtado A, Aljabali AAA, Mishra V, Tambuwala MM, Serrano-Aroca Á. Alginate: Enhancement Strategies for Advanced Applications. Int J Mol Sci [Internet]. 2022 May [cited 2023 Apr 12];23(9). Available from: http://www.ncbi.nlm.nih.gov/pmc/articles/PMC9102972/

67. Rhein-Knudsen N, Ale MT, Ajalloueian F, Meyer AS. Characterization of alginates from Ghanaian brown seaweeds: Sargassum spp. and Padina spp. Food Hydrocoll. 2017 Oct;71:236–44.

68. Trica, Delattre, Gros, Ursu, Dobre, Djelveh, et al. Extraction and Characterization of Alginate from an Edible Brown Seaweed (Cystoseira barbata) Harvested in the Romanian Black Sea. Mar Drugs. 2019 July 8;17(7):405.

69. Moradali MF, Donati I, Sims IM, Ghods S, Rehm BH. Alginate polymerization and modification are linked in Pseudomonas aeruginosa. MBio. 2015;6(3):10–1128.

70. Mathlouthi M, Koenig JL. Vibrational spectra of carbohydrates. Adv Carbohydr Chem Biochem. 1987;44:7–89.

71. Fenoradosoa TA, Ali G, Delattre C, Laroche C, Petit E, Wadouachi A, et al. Extraction and characterization of an alginate from the brown seaweed Sargassum turbinarioides Grunow. J Appl Phycol. 2010;22:131–7.

72. Papageorgiou SK, Kouvelos EP, Favvas EP, Sapalidis AA, Romanos GE, Katsaros FK. Metal–carboxylate interactions in metal–alginate complexes studied with FTIR spectroscopy. Carbohydr Res. 2010;345(4):469–73.

73. Leal D, Matsuhiro B, Rossi M, Caruso F. FT-IR spectra of alginic acid block fractions in three species of brown seaweeds. Carbohydr Res. 2008 Mar 1;343:308–16.

74. Gómez-Ordóñez E, Rupérez P. FTIR-ATR spectroscopy as a tool for polysaccharide identification in edible brown and red seaweeds. Food Hydrocoll. 2011 Aug 1;25(6):1514–20.

75. Avella M, Di Pace E, Immirzi B, Impallomeni G, Malinconico M, Santagata G. Addition of glycerol plasticizer to seaweeds derived alginates: Influence of microstructure on chemical–physical properties. Carbohydr Polym. 2007;69(3):503–11.

76. Ji D, Park JM, Oh MS, Nguyen TL, Shin H, Kim JS, et al. Superstrong, superstiff, and conductive alginate hydrogels. Nat Commun. 2022;13(1):3019.

77. Liu S, Li Y, Li L. Enhanced stability and mechanical strength of sodium alginate composite films. Carbohydr Polym. 2017 Mar 15;160:62–70.

78. Li J, Wu Y, He J, Huang Y. A new insight to the effect of calcium concentration on gelation process and physical properties of alginate films. J Mater Sci. 2016 June;51(12):5791–801.

79. Janik W, Nowotarski M, Ledniowska K, Shyntum DY, Krukiewicz K, Turczyn R, et al. Modulation of physicochemical properties and antimicrobial activity of sodium alginate films through the use of chestnut extract and plasticizers. Sci Rep. 2023 July 17;13(1):11530.

View Article Online
DOI: 10.1039/D5GC05514H

80. Hambleton A, Perpiñan-Saiz N, Fabra MJ, Voilley A, Debeaufort F. The Schroeder paradox or how the state of water affects the moisture transfer through edible films. 6th Int Conf Water Food. 2012 June 15;132(4):1671–8.

81. Can Karaca A, Erdem IG, Ak MM. Effects of polyols on gelation kinetics, gel hardness, and drying properties of alginates subjected to internal gelation. LWT. 2018 June 1;92:297–303.

82. Anbinder PS, Deladino L, Navarro AS, Amalvy JI, Martino MN. Yerba mate extract encapsulation with alginate and chitosan systems: interactions between active compound encapsulation polymers. J Encapsulation Adsorpt Sci. 2011;1(4):80–7.

83. Abulateefeh SR, Taha MO. Enhanced drug encapsulation and extended release profiles of calcium–alginate nanoparticles by using tannic acid as a bridging cross-linking agent. J Microencapsul. 2015;32(1):96–105.

84. Azucena Castro-Yobal M, Contreras-Oliva A, Saucedo-Rivalcoba V, Rivera-Armenta JL, Hernández-Ramírez G, Salinas-Ruiz J, et al. Evaluation of physicochemical properties of film-based alginate for food packing applications. E-Polym. 2021;21(1):82–95.

85. Mamun A, Rahman SM, Roland S, Mahmood R. Impact of molecular weight on the thermal stability and the miscibility of poly (ε-caprolactone)/polystyrene binary blends. J Polym Environ. 2018;26(8):3511–9.

86. Benavides S, Villalobos-Carvajal R, Reyes J. Physical, mechanical and antibacterial properties of alginate film: Effect of the crosslinking degree and oregano essential oil concentration. J Food Eng. 2012;110(2):232–9.

87. Santana A, Kieckbusch T. Physical evaluation of biodegradable films of calcium alginate plasticized with polyols. Braz J Chem Eng. 2013;30:835–45.

88. Crossingham YJ, Kerr PG, Kennedy RA. Comparison of selected physico-chemical properties of calcium alginate films prepared by two different methods. Int J Pharm. 2014 Oct 1;473(1):259–69.

89. Li J, He J, Huang Y, Li D, Chen X. Improving surface and mechanical properties of alginate films by using ethanol as a co-solvent during external gelation. Carbohydr Polym. 2015 June 5;123:208–16.

90. Abka-Khajouei R, Tounsi L, Shahabi N, Patel AK, Abdelkafi S, Michaud P. Structures, properties and applications of alginates. Mar Drugs. 2022;20(6):364.

91. Olivas GI, Barbosa-Cánovas GV. Alginate–calcium films: Water vapor permeability and mechanical properties as affected by plasticizer and relative humidity. LWT - Food Sci Technol. 2008 Mar;41(2):359–66.

92. Manikandan G, Senthilkumar G, Chen CW, Nagarajan D, Chang JS, Dong CD. Valorization of brown seaweed into next-generation alginate bioplastic films: Functional enhancements and smart packaging applications. Carbohydr Polym. 2025 Dec 15;370:124356.

93. Hao J, Yan S, Yuan H, Du C, Tan Y. High-strength alginate fibers wet-spun from pre-crosslinked sodium alginate solutions. Carbohydr Polym. 2024 Oct 15;342:122386.

94. Qin Y. Alginate fibres: an overview of the production processes and applications in wound management. Polym Int. 2008;57(2):171–80.

View Article Online
DOI: 10.1039/D5GC05514H

95. Swetha TA, Bora A, Mohanrasu K, Balaji P, Raja R, Ponnuchamy K, et al. A comprehensive review on polylactic acid (PLA) – Synthesis, processing and application in food packaging. Int J Biol Macromol. 2023 Apr 15;234:123715.

96. Xie F, Gao C, Avérous L. Alginate-based materials: Enhancing properties through multiphase formulation design and processing innovation. Mater Sci Eng R Rep. 2024;159:100799.

97. Mohammed A, Ward K, Lee KY, Dupont V. The environmental impact and economic feasibility assessment of composite calcium alginate bioplastics derived from Sargassum. Green Chem. 2023;25(14):5501–16.

View Article Online
DOI: 10.1039/D5GC05514H

Data availability statement

The authors confirm that the data supporting the findings of this study are available within the article and its Supplementary Information (SI), which includes additional figures (normality assessment, preliminary extraction trials, and M/G-yield correlation), and environmental assessment data, sources, assumptions and calculations for optimized and non-optimized citrate extractions.